View metadata, citation and similar papers at core.ac.uk

brought to you by CORE

provided by Elsevier - Publisher Connector

FEBS Letters 585 (2011) 2599–2603

FEBS Letters

journal homepage: www.FEBSLetters.org

Ligand entry pathways in the ligand binding domain of PPARγ receptor

Samia Aci-Sèche, Monique Genest, Norbert Garnier *

Centre de Biophysique Moléculaire, UPR 4301 – Affiliated to the University of Orléans, CNRS, rue Charles Sadron, 45071 Orléans Cedex 02, France

ARTICLE INFO

Article history:
Received 4 May 2011
Revised 29 June 2011
Accepted 11 July 2011
Available online 22 July 2011

Edited by Robert B. Russell

Keywords:
Targeted molecular dynamics
Ligand entry pathway
PPARγ

ABSTRACT

To address the question of ligand entry process, we report targeted molecular dynamics simulations of the entry of the flexible ionic ligand GW0072 in the ligand binding domain of the nuclear receptor PPARγ. Starting with the ligand outside the receptor the simulations led to a ligand docked inside the binding pocket resulting in a structure very close to the holo-form of the complex. The results showed that entry process is guided by hydrophobic interactions and that entry pathways are very similar to exit pathways. We suggest that TMD method may help in discriminating between ligands generated by in silico docking.

© 2011 Federation of European Biochemical Societies. Published by Elsevier B.V. All rights reserved.

1. Introduction

Docking is an in silico structure-based drug design technique used to select ligands with the best affinity for the binding site of a given receptor. Generally this is achieved by searching the most favourable orientation of each member of a set of molecules within a rigid binding site with the most favourable stability. Ligands having good affinity are called positive ligands contrarily to those having bad affinity which are called negative ligands. Current docking programs (for a list of some docking programs see [1]) take ligand flexibility into account while the receptor is considered rigid or partially rigid, allowing side chain flexibility. The risk of neglecting receptor flexibility is the determination of false negative ligands. Simulation methods such as Molecular Dynamics (MD) and Normal Modes analysis (NM) may improve the search for potentially active ligands, but the question of the pathway for the ligand to reach the binding site within the receptor is not addressed. Nevertheless, the knowledge of ligand pathways represents an important component of ligand affinity, since high energy barriers may prevent the ligand from reaching the binding site, thus leading to false positive ligands being defined.

The determination of ligand entry pathways is a difficult task, both experimentally and computationally. Simulation studies have proved helpful in finding pathways for a ligand to escape from a receptor [2–6], but only a few studies deal with ligand entry pathways [7–10]. Obviously, escape and entry pathways are a priori not identical.

To address the question of the ligand entry process, we report here Targeted Molecular Dynamics (TMD) simulations of the binding of the GW0072 ligand with the ligand binding domain (LBD) of the Peroxysome Proliferator-Activated Receptor gamma (PPARγ). This receptor from the superfamily of nuclear receptor is a pharmacological target for a number of diseases [11]. We were motivated to study this complex because (i) GW0072 is a large ionic highly flexible ligand including aliphatic and polar groups [12], and (ii) previous simulations have defined possible escape pathways for this ligand [6]. Starting from the apo-form of the receptor (PDB.ID 1PRG, A chain) [13] with the ligand located outside, TMD simulations converge close to the targeted structure of the holo-form of the complex (PDB.ID 4PRG, A chain) [12] defining a penetration pathway into the binding pocket that is very similar to escape pathways [6].

2. Methods

All the simulations were performed in the presence of explicit water molecules and Na+ counterions using the parallelized version of the SANDER program from the AMBER 9.0 package [14]. The simulation protocol follows that described in our previous study [6] and is given in Supplementary material (Text T1).

In TMD simulation, a group of atoms is guided from an initial structure toward a target structure by decreasing step by step the root mean square deviation (RMSD) between the two structures [15]. In this study the initial structure of the receptor is the X-ray structure of the apo-form of the LBD of PPARγ (PDB.ID 1PRG, A Chain [13]). The initial conformation of GW0072 was generated by a conformational search using MacroModel and placed near gate A identified previously as the most probable exit gate [6] and also because

* Corresponding author.
E-mail addresses: samia.aci@cnrs-orleans.fr (S. Aci-Sèche), monique.genest@cnrs-orleans.fr (M. Genest), norbert.garnier@cnrs-orleans.fr (N. Garnier).

0014-5793/$36.00 © 2011 Federation of European Biochemical Societies. Published by Elsevier B.V. All rights reserved.
doi:10.1016/j.febslet.2011.07.014

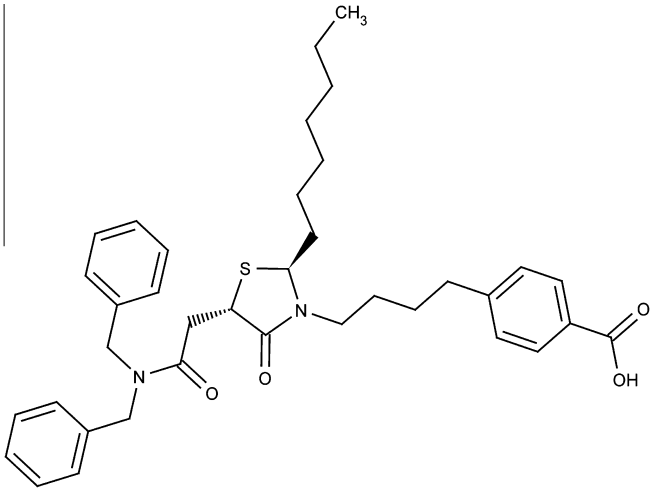

Fig. 1. Chemical structure of the GW0072 ligand.

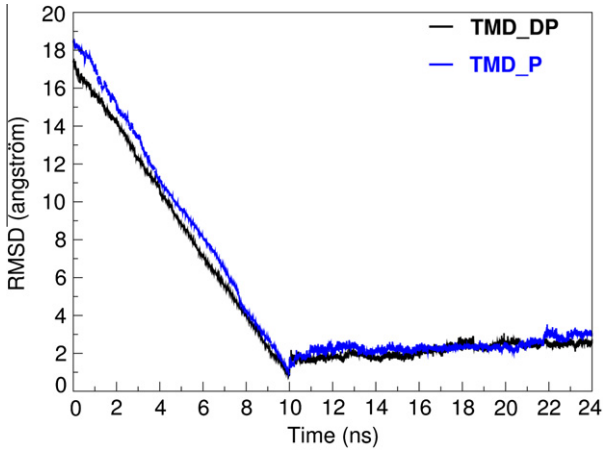

Fig. 2. Time evolution of the RMSD calculated on the backbone heavy atoms of the binding site and all the atoms of the ligand, relative to the targeted structure: TMD_DP (black) and TMD_P (blue).

it is the potential entry gate proposed by Nolte et al. [13]. But we keep in mind that other gates could exist. The targeted structure is the X-ray structure of PPARγ bound to the GW0072 ligand (PDB.ID 4PRG, A chain [12]). Because of uncertainties on proton exchange during ligand entry, two distinct simulations were conducted, one with the protonated form of GW0072 (TMD_P) (carboxyl protonated head, Fig. 1) and the other one with the deprotonated form (TMD_DP). Constraints were applied on all the ligand atoms and on the backbone heavy atoms of the residues of the binding site that were defined as the residues having at least one atom separated by less than 3.5 Å from any atom of the ligand in the holo form of PPARγ. The remainder of the protein was not restrained.

After minimization, heating and equilibration at 300 K, the RMSD on the set of selected atoms calculated between the equilibrated conformation and the target were 17.4 Å and 18.5 Å for TMD_DP and TMD_P, respectively. During TMD simulation, the RMSD value was constrained to decrease progressively by steps of 0.085 Å and 0.09 Å, respectively, every 50 ps and was approximately 0.4 Å and 0.5 Å after 10 ns. This was followed by 14 ns of free simulation for system relaxation.

The RMSD and atomic fluctuations were monitored using the PTRAJ program. Hydrogen bond occupancy was calculated using the HBonds plugin included in the Visual Molecular Dynamics software (VMD) [16] using a 3.2 Å cut-off for the donor–acceptor distance and a donor-hydrogen-acceptor angle lower than 65°. Energy calculations were performed with the MM-PBSA module and protein–ligand hydrophobic interactions were analysed and visualized using Ligplot [17]. A maximal separation of 3.9 Å between the two atoms is used to define these hydrophobic interactions.

3. Results

TMD_P and TMD_DP both successfully led to the formation of a stable protein–ligand complex. During the 14 ns of free simulations the ligand remained docked inside the binding site. A continuous decrease in the RMSD was observed during the TMD period (Fig. 2) along with a weak constrained energy (lower than 10 kcal/mol except for the last 500 ps). During the relaxation period, the RMSD stabilized around 2–3 Å.

3.1. Energetics

Fig. 3 shows the evolution of the interaction energies between the ligand and the receptor during the entry process (0–10 ns) and the relaxation period (10–24 ns). During the entry process

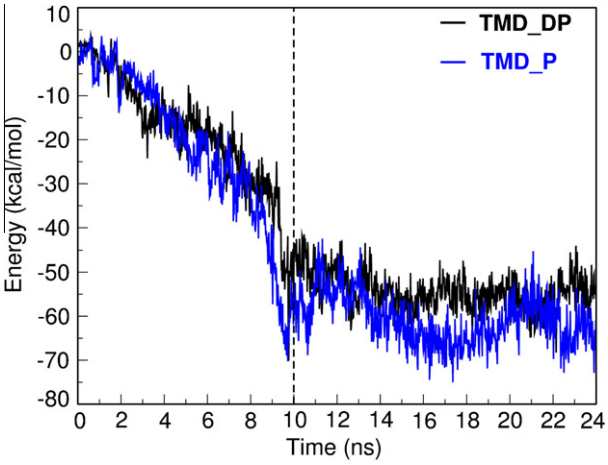

Fig. 3. Interaction energies between the ligand and the receptor in TMD_DP (black) and TMD_P (blue) simulations.

the energy value continuously decreases from 0 kcal mol^{-1} to about −55 kcal mol^{-1}. Interestingly, for both ligand states, no energy barrier was detected until the ligand reaches the binding site (0–9.5 ns). After 8 ns, the alkyl chain and the aromatic core are placed in the binding site. Then, the positioning of the polar head leads to an energetic drop (8–9.5 ns). For the last 0.5 ns (9.5–10 ns) the constraints applied on the ligand to adjust the target conformation results in a small energetic rise. In the course of the relaxation period (10–24 ns), the interaction energy fluctuates around the mean value −61 kcal mol^{-1} (TMD_P) or −53 kcal mol^{-1} (TMD_DP). This energy is slightly more favourable for the protonated ligand than for the deprotonated one.

3.2. Internal dynamics during TMD simulations

The internal dynamics of the receptor during the entry process is revealed by the fluctuations of the Cα atom positions as shown in Fig. 4. Several high peaks evidence large atomic fluctuations (excluding end effects). The highest peaks involve the loop joining helix H2 and the first strand S1 of the β sheet, helix H2′ and the H2′–H3 loop. These two peaks were observed in both simulations. Two lower peaks correspond to the loops joining the two helices H8 and H9 and helices H9 and H10/H11. Another region with moderate fluctuations containing H5′ and H6 and the S3 and S4

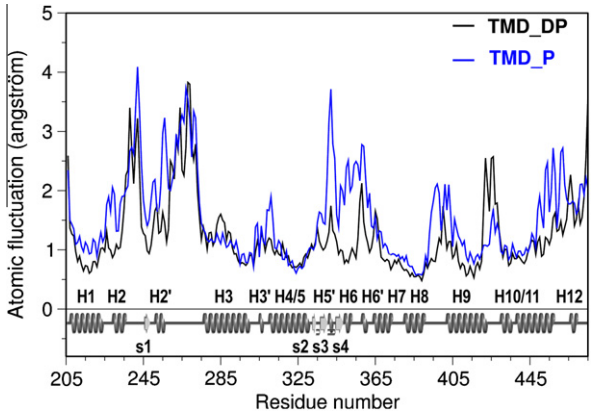

Fig. 4. Cα atomic fluctuations during the 10 ns TMD period of the TMD_DP (black) and TMD_P (blue) simulations.

β-strands was observed only in TMD_P. These flexible regions are shown in Fig. 5. Interestingly, these regions overlap the border of gate A pointed out during the exit pathway process [6].

3.3. Entry/exit pathways

The two ligand entry pathways determined in the present study and the probable ligand escape pathways [6] are compared in Fig. 6. It can be seen that the ligand entry routes are very similar to five of the six exit pathways through gate A, regardless of the ligand protonation state. There is, however, a difference in the vicinity of the H5′ helix. In TMD_DP, the ligand avoids H5′ to find the best route, while during TMD_P, helix H5′ is pushed away by the ligand and partially loses its helical structure, allowing ligand entry. Once the ligand enters the binding site, H5′ recovers its helical structure which remains stable throughout the 14 ns of the relaxation period. The role played by this helix in the closing gate process was already revealed in our ligand escape pathway study [6].

During the first steps of the entry process, the ligand rotates on itself in order to guide the hydrophobic region close to the entry site. In both simulations it is observed that the alkyl chain tends to enter first, coming into contact with helix H5′. In TMD_DP this small helix is easily bypassed by the alkyl chain followed by the benzyl groups. On the contrary, in TMD_P, the alkyl group is blocked until the benzyl groups first bypass H5′, driving thereafter the alkyl chain deeper into the protein. In both cases, the carboxylic polar head remains in contact with the solvent as long as possible.

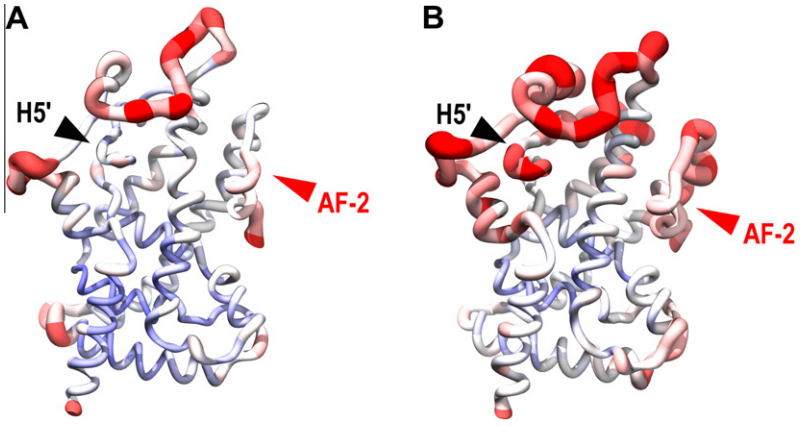

Fig. 5. Worm representation of the flexible regions of LBD PPAR observed during the TMD phase: (A) TMD_DP; (B) TMD_P. Residues with low atomic fluctuations are in blue and residues with high atomic fluctuations are in red.

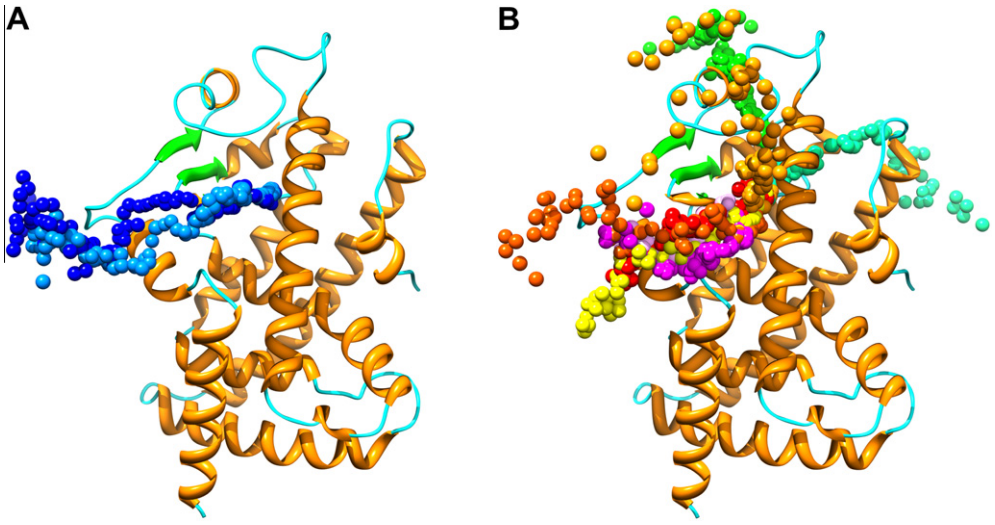

Fig. 6. (A) Ligand entry pathways determined from TMD_DP (sky blue) and TMD_P (deep-blue) and (B) escape pathways described in [6].

3.4. Protein–ligand interactions

Table 1 summarizes the protein–ligand hydrophobic interactions of the most central structure of the complex for both forms of the ligand during the relaxation period. For comparison, the 18 hydrophobic interactions detected in the X-ray structure of the complex (4PRG chain A) are also reported. Only 10 of these interactions were detected in the central structure generated by TMD_P and 8 in the case of TMD_DP. Six are shared by the X-ray structure and the TMD_P and TMD_DP central structures. Residues in interaction with the aromatic core of GW0072 are remarkably well conserved in both simulations, contrarily to the residues interacting with the aliphatic and carboxyphenyl groups. Indeed, as shown in Fig. 7, the positions of the aromatic core in the three structures are well superimposed and located in the hydrophobic pocket.

Table 1
Protein–ligand hydrophobic interactions in the X-ray structure and in the central structure of the TMD_DP and TMD_P relaxation period. Interactions with the aromatic core are in bold: those common to the three structures are labeled ∗, others are in italics.

4PRG (X-ray)	TMD_P	TMD_DP
Leu255	–	–
–	–	Ile262
Phe264	Phe264	–
His266	His266	–
Ala278	–	–
Arg280	–	–
Ile281	Ile281	–
Cys285∗	**Cys285**∗	**Cys285**∗
Arg288∗	**Arg288**∗	**Arg288**∗
Ile326	***Ile326***	–
Tyr327∗	**Tyr327**∗	**Tyr327**∗
Met329∗	**Met329**∗	**Met329**∗
Leu330∗	**Leu330**∗	**Leu330**∗
Leu333∗	**Leu333**∗	**Leu333**∗
	–	***Val339***
Ile341	–	***Ile341***
Leu356	–	–
Phe360	–	–
Phe363	–	–
Met364	–	Met364
–	His449	–

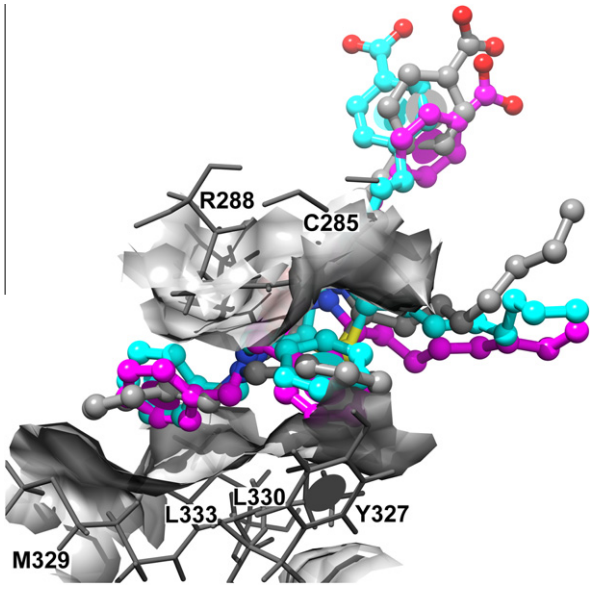

Fig. 7. Superimposition of the central structures calculated from the relaxation period for the TMD_DP (cyan) and TMD_P simulations (pink) onto the X-ray structure (gray).

Table 2
Hydrogen bonds observed in the course of TMD_DP and TMD_P compared to the hydrogen bonds in the X-ray structure.

Hbond donor	Hbond acceptor	4PRG (X-ray)	TMD_DP	TMD_P
Ser342	GW0072	100	12.9	0.7
Arg288	GW0072	100	0.6	0.3
GW0072	Glu259	0	0.0	0.0
Arg280	GW0072	0	0.0	87.8
Lys263	GW0072	0	46.5	0.0
GW0072	Leu255	0	0.0	61.3
Cys285	GW0072	0	3.7	4.3

Protein–ligand H-bonds have been also analyzed and are given in Table 2. The two intermolecular H-bonds present in the X-ray structure, involving Ser342 and Arg288, are seen as very transitory events during the two simulations. One major H-bond was detected in the TMD_DP simulation, present during 47% of the relaxation time and involving Lys263. Two important H-bonds are highlighted in the TMD_P simulation occurring for 88% and 61% of the relaxation time and involving Arg280 and Leu255, respectively.

3.5. Discussion and conclusion

Simulation methods are proved helpful to describe ligand escape pathways from their binding site located in a protein pocket [2–6], but very few studies have addressed the ligand entry process into receptors. The present work aimed to tackle this point which is rather difficult when considering the large and flexible ligand GW0072, a 90-atom molecule containing a carboxyl head, an aliphatic chain and an aromatic core (Fig. 1) and its receptor, the LBD of PPARγ. The X-ray structures of the protein with and without the ligand are available in the Protein Data Bank (www.pdb.org [18]) and exit pathways were determined from MD simulations [6].

In this work we evidence two very similar entry pathways for GW0072 using TMD simulations and we focus on two aspects: (i) the similarity or the difference of entry/exit pathways; (ii) the presence of energy barriers during the entry process. The influence of the protonation state of GW0072 has also been investigated. Using the TMD approach [15] the initial system including the apo-form of the receptor and the ligand outside was targeted on the X-ray structure of the holo-form of the complex. The two simulations carried out with the protonated and deprotonated forms of the ligand led to the formation of a stable complex although the orientation of the ligand polar heads differed in the binding pocket. Entry pathways were found identical for the two states of the ligand without an energy barrier during the entry process. A very interesting result is that these entry pathways are very similar to the main exit pathway described in our previous study [6]. Of course, this finding may be different for other receptors and other ligands.

Both the motion of the ligand before entering the receptor for guiding first the hydrophobic part at the entry gate and the way the ligand finally anchors in the hydrophobic pocket strongly suggest that the entry process in LBD is mainly governed by hydrophobic interactions. However, polar interactions play a role in the stabilization of the ligand. Two strong H-bonds involving Leu255 and Arg280 are observed in TMD_P while a unique weak H-bond involving Lys263 is observed in TMD_DP. Thus, the protonated form of the ligand is slightly more stable than the deprotonated form and this difference in stability could be related to the desolvation of the carboxyl head of the ligand which could be a rate limiting step of the ligand insertion [9].

It is also important to note the very different behaviour of helix AF-2 during the entry phase and the relaxation phase. Obviously, there is no direct interaction between GW0072 and AF-2 during

the ligand entry process. But while GW0072 enters the receptor (Fig. 5) the helix is very mobile and once the ligand is placed in the pocket AF-2 becomes much less flexible during the rest of the simulation (Fig. S1 in Supplementary material). This finding is in good agreement with the observation of Oberfield et al. [12] suggesting that although there is no direct interactions with the ligand, its presence in the binding site stabilizes AF-2 in an intermediate conformation which could be responsible of the properties of partial agonist for GW0072.

In this work we have shown that TMD can drive the GW0072-PPARγ system from an unbound form to the bound form. Starting with the ligand outside the receptor, the simulations led to a ligand docked inside the binding pocket, resulting in a structure very close to that of an a priori known structure. However, the question arises whether the same result would be obtained if the structure of the complex were unknown. To answer this question, complementary MD simulations, starting from the same initial complex, were performed during which the distance between the centers of mass of the ligand and of the binding site was progressively constrained to decrease (not detailed here). This simulation successfully led to a final structure close to the holo-form of the complex (PDB.ID 4PRG) and the ligand entry pathway was globally superimposed on that found from TMD simulations.

The results reported here are encouraging and suggest that the TMD method is helpful in discriminating between ligands generated by in silico docking. It can be considered that a molecule with high affinity related to strong binding site interactions and therefore declared as an agonist or antagonist candidate would be eliminated if its entry pathway into the receptor evidences high energy barriers.

Acknowledgements

We gratefully acknowledge the Region Centre (France) for financial support. The technical assistance of A. Boyer is greatly appreciated.

Appendix A. Supplementary data

Supplementary data associated with this article can be found, in the online version, at doi:10.1016/j.febslet.2011.07.014.

References

[1] Moitessier, N., Englebienne, P., Lee, D., Lawandi, J. and Corbeil, C.R. (2008) Towards the development of universal, fast and highly accurate docking/scoring methods: a long way to go. Br. J. Pharmacol. 153 (Suppl. 1), S7–S26.
[2] Yang, L.J., Zou, J., Xie, H.Z., Li, L.L., Wei, Y.Q. and Yang, S.Y. (2009) Steered molecular dynamics simulations reveal the likelier dissociation pathway of imatinib from its targeting kinases c-Kit and Abl. PLoS One 4, e8470.
[3] Wang, T. and Duan, Y. (2009) Ligand entry and exit pathways in the beta2-adrenergic receptor. J. Mol. Biol. 392, 1102–1115.
[4] Perakyla, M. (2009) Ligand unbinding pathways from the vitamin D receptor studied by molecular dynamics simulations. Eur. Biophys. J. 38, 185–198.
[5] Kalikka, J. and Akola, J. (2010) Steered molecular dynamics simulations of ligand–receptor interaction in lipocalins. Eur. Biophys. J. 40, 181–194.
[6] Genest, D., Garnier, N., Arrault, A., Marot, C., Morin-Allory, L. and Genest, M. (2008) Ligand-escape pathways from the ligand-binding domain of PPARgamma receptor as probed by molecular dynamics simulations. Eur. Biophys. J. 37, 369–379.
[7] Hurst, D.P., Grossfield, A., Lynch, D.L., Feller, S., Romo, T.D., Gawrisch, K., Pitman, M.C. and Reggio, P.H. (2010) A lipid pathway for ligand binding is necessary for a cannabinoid G protein-coupled receptor. J. Biol. Chem. 285, 17954–17964.
[8] Martinez, L., Polikarpov, I. and Skaf, M.S. (2008) Only subtle protein conformational adaptations are required for ligand binding to thyroid hormone receptors: simulations using a novel multipoint steered molecular dynamics approach. J. Phys. Chem. B 112, 10741–10751.
[9] Friedman, R., Nachliel, E. and Gutman, M. (2005) Molecular dynamics simulations of the adipocyte lipid binding protein reveal a novel entry site for the ligand. Biochemistry 44, 4275–4283.
[10] Shan, Y., Kim, E.T., Eastwood, M.P., Dror, R.O., Seeliger, M.A. and Shaw, D.E. (2011) How does a drug molecule find its target binding site? J. Am. Chem. Soc. 133, 9181–9183.
[11] Fogo, A.B. (2011) PPARgamma and chronic kidney disease. Pediatr. Nephrol. 26, 347–351.
[12] Oberfield, J.L. et al. (1999) A peroxisome proliferator-activated receptor gamma ligand inhibits adipocyte differentiation. Proc. Natl. Acad. Sci. USA 96, 6102–6106.
[13] Nolte, R.T. et al. (1998) Ligand binding and co-activator assembly of the peroxisome proliferator-activated receptor-gamma. Nature 395, 137–143.
[14] Case, D.A. et al. (2006) AMBER, 9ed., University of California, San Francisco.
[15] Schlitter, J., Engels, M. and Kruger, P. (1994) Targeted molecular dynamics: a new approach for searching pathways of conformational transitions. J. Mol. Graph. 12, 84–89.
[16] Humphrey, W., Dalke, A. and Schulten, K. (1996) VMD: visual molecular dynamics. J. Mol. Graph. 14 (33–8), 27–28.
[17] Wallace, A.C., Laskowski, R.A. and Thornton, J.M. (1995) LIGPLOT: a program to generate schematic diagrams of protein–ligand interactions. Protein Eng. 8, 127–134.
[18] Berman, H.M., Westbrook, J., Feng, Z., Gilliland, G., Bhat, T.N., Weissig, H., Shindyalov, I.N. and Bourne, P.E. (2000) The protein data bank. Nucleic Acids Res. 28, 235–242.